Low-Threshold 3 µm GaInAsSb/AlGaInAsSb Quantum-Well Lasers Operating in Continuous-Wave up to 64 °C

Kristijonas Vizbaras, Alexander Andrejew, Augustinas Vizbaras, Christian Grasse, Shamsul Arafin, and Markus-Christian Amann
Walter Schottky Institut, Technische Universität München, Am Coulombwall 3, 85478 Garching, Germany
E-Mail: Kristijonas.Vizbaras@wsi.tum.de

Abstract

Long-wavelength lasers, emitting above 2 µm, are attractive light sources for trace-gas sensing systems with tunable diode-laser absorption spectroscopy (TDLAS). Here, GaSb-based lasers are perfectly suited, as they can cover the spectral range from 2 to 4 µm. Many technologically important gases, such as CO, CO_2, CH_4, NH_3, N_2O, etc., have strong absorption lines in this region. The spectral range around 2.9 - 3.0 µm is of specific interest for NH_3 and N_2O sensing applications. In this work, we present state-of-the-art GaInAsSb/AlGaInAsSb quantum-well (QW) ridge-waveguide lasers emitting around 3 µm. Episide-up mounted devices operate in continuous wave (CW) with very low threshold current densities up to record-high 64 °C heatsink temperature. This is by ~20 °C higher, than the best reported value of 45 °C for episide-down indium-soldered devices at this wavelength range. In pulsed mode devices were operating beyond 80 °C heatsink temperature, limited only by the characterization set-up. Extrapolated pulsed threshold currents at 20 °C for infinite resonator length (L→∞) yield 168 A/cm^2 for 3 QW active region, corresponding to only 56 A/cm^2 per QW. In CW operation the extrapolated (L→∞) threshold current was found to be 198 A/cm^2, yielding 66 A/cm^2 per QW. For this long wavelength range, a very high characteristic temperature (T_0) of 43 K was determined in the temperature range of 10 to 60 °C.

1 Introduction

Long-wavelength lasers, emitting above 2 µm, are attractive light sources for trace-gas sensing systems with tunable diode-laser absorption spectroscopy (TDLAS) [1]. Here, GaSb-based lasers are perfectly suited, as they can cover the spectral range from 2 to 4 µm. Many technologically important gases, such as CO, CO_2, CH_4, NH_3, etc., have strong absorptions lines in this region [2]. The spectral region around 2.9 µm is of particular interest for NH_3 sensing applications. However, several problems arise with increasing laser emission wavelength. Carrier loss mechanisms, such as Auger recombination and inter-valence band absorption rapidly increase. Moreover, epitaxial growth of quantum-well (QW) material for longer wavelengths gets complicated: *in-situ* annealing effects [3-5] during growth, which lead to a significant increase of bandgap energy and material deterioration become critical. Also, one has to increase the In concentration to lower the transition energy, which brings the material deeper into the miscibility gap [6] and makes it more difficult to grow. Additionally, increasing indium content reduces the valence band offset and a proper barrier material has to be chosen to maintain type-I band alignment, which is needed for hole confinement in the wells.. Typically, the material of choice is either quaternary AlGaAsSb or quinternary AlGaInAsSb, as GaSb barriers cannot provide sufficient hole confinement anymore.

In this work we present lasers with 3 GaInAsSb QWs embedded in quinternary AlGaInAsSb barrier layer. Lasers operate in CW around 3µm up to record-high 64 °C and exhibit very low threshold current densities, like 66 A/cm^2 per QW for infinite length, at 20 °C.

2 Device fabrication

2.1 Design and epitaxial growth

The device structures were grown on *n*-GaSb substrates in a solid source Varian Mod Gen – II MBE system equipped with valved cracker cells for antimony and arsenic. The temperature is determined by means of optical pyrometry, which is calibrated to the GaSb oxide desorption temperature ~ 550 °C. The growth starts with a 2500 nm thick $Al_{0.5}Ga_{0.5}As_{0.04}Sb$ *n*-cladding layer grown at 500°C. Here, the first 1500 nm were nominally doped to the level of $5\times10^{17}\,cm^{-3}$ and the remaining 1000 nm were doped to $1\times10^{17}\,cm^{-3}$ to reduce the losses due to free-carrier absorp-

ISBN 978-3-8007-3356-9

tion. The cladding is followed by the growth of a waveguide layer, which also serves as a separate confinement layer. For the waveguide material 275 nm thick quaternary $Al_{0.15}Ga_{0.85}As_{0.02}Sb_{0.98}$ was chosen. In order to reduce the voltage drop, but still keep the free-carrier losses low in this high-bandgap (0.91 eV) material, the waveguide was doped in the following manner: the first 100 nm were Te doped to the level of $5\times10^{16}\,cm^{-3}$ and the remaining 175 nm had a Te doping of $2\times10^{16}\,cm^{-3}$. Next, the active region is grown at a temperature of 460 °C. We chose three compressively strained (1.43% relaxed strain) 10nm wide $Ga_{0.57}In_{0.43}As_{0.18}Sb_{0.82}$ QWs embedded in 10 nm wide digitally alloyed quinternary $Al_{0.16}Ga_{0.61}In_{0.23}As_{0.22}Sb_{0.78}$ barriers. The latter well-barrier combination resulted in type – I band alignment with 147 meV confinement for the electrons and 71 meV confinement for heavy holes, calculated from the first quantized states. The schematic band diagram is presented in Fig. 1. All calculations were carried out using material parameters from [7] and quaternary alloy bowing parameters were from [8].

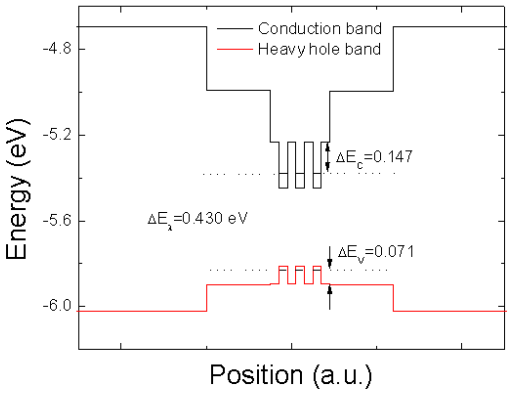

Figure 1 Simulated schematic energy-band diagram of the active region in the laser.

After the active region, the nominally undoped 275 nm thick $Al_{0.15}Ga_{0.85}As_{0.02}Sb_{0.98}$ waveguide was grown, which was followed by a Si doped 2500 nm thick $Al_{0.5}Ga_{0.5}As_{0.04}Sb$ *p*-cladding layer. The layer was doped in a similar manner as the *n*-cladding: the first 1 µm had a doping level of $1\times10^{17}\,cm^{-3}$ and the remaining 1.5 µm had a doping of $5\times10^{17}\,cm^{-3}$. The structure was finished with a 50 nm thick heavily doped ($1\times10^{19}\ cm^{-3}$) *p*-GaSb contact layer.

2.2 Device fabrication and characterization

Ridge-waveguide lasers with stripe widths from 3 to 30 µm were processed by dry chemical etching of the *p*-cladding layer and stopping in the waveguide before the active region. For mesa passivation, sputtered SiO_2 was used and for *p*- and *n*- metallization Ti/Pt/Au contacts have been evaporated. The lasers were cleaved into laser bars of different lengths (from 500 µm to 4mm) and were mounted episide-up on copper heat sinks. For threshold current density evaluation in CW and pulsed mode no facet coating has been applied. For maximum operation temperature evaluation in CW mode, high-reflective (HR) coatings of 95 % reflectivity have been applied on one facet. The other facet was left as cleaved (AC). All measurements have been carried out on a temperature controlled stage. All pulsed measurements have been carried out using 500 ns pulse length, with a repetition frequency of 1kHz. The temperature values given in this paper correspond to heat sink temperature, measured with a thermopile, and are uncorrected for internal heating of the device.

3 Device results and discussion

Figure 2 shows a semi-log plot of pulsed threshold current density as a function of inverse cavity length. Lasers exhibit very low threshold current densities, corresponding to an extrapolated value of 56 A/cm^2 per QW, at infinite resonator length. Current broadening of 8.8 µm on both sides has been extracted from threshold current dependence on mesa width and the validity of the estimate was proved by a good overlap of the threshold current densities for devices with different mesa widths. From threshold current – temperature dependence a high characteristic temperature T_0 value of 43 K has been extracted (see inset in Fig. 2). This value is by 20% to 30% better than recently reported values for this wavelength range [9-11] (see Table 1). We attribute such a better performance to a relatively strong heavy hole confinement of 71 meV achieved with our barrier-well material combination. In comparison, devices in [11] had a confinement for holes of only 20 meV.

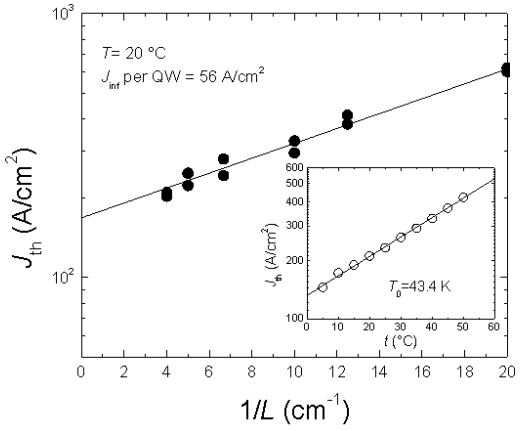

Figure 2 Pulsed threshold current density as a function of inverse cavity length at 20°C for devices with mesa width of 30 µm. The inset shows threshold current density as a function of heatsink temperature under pulsed operation for a 1 mm long device with 10 µm wide ridge. Exponential fit of the data gives the characteristic temperature of 43 K.

In addition to low-thresholds and good characteristic temperature, devices also exhibit a very large operation temperature range. The maximum operating temperature under

ISBN 978-3-8007-3356-9

pulsed operation was found to be above 80 °C, what is limited by the measuring set-up and not the device itself. This is much higher than values of 55 °C [9-10] and 50 °C [11] reported up to now (see Table 1).

TABLE I
DEVICE PROPERTIES

Parameter	3QW laser (This work)	2QW laser [11]	2QW laser [12-13]	2QW laser [10]
λ (μm)	2.9-3.0	3.0	3.1	2.9-3.0
T_0 (K)	43	30	-	34
$T_{max.}$ CW (°C)	64	30	45	38
$T_{max.}$ (pulsed) (°C)	>80	50	-	55
J_{th} per QW, CW (A/cm^2) at RT	155	595	163*	562**
L (mm)	1	1.8	2	1.2

Table 1 Device properties of GaInAsSb QW lasers, emitting around 3 μm. Here λ is the emission wavelength of the laser, J_{th} is threshold current density, T_0 is characteristic temperature, T_{max} is the maximum operation temperature and L is the cavity length. *This device had HR/AC coatings on mirrors and was mounted episide-down; **the threshold current is for a DFB laser.

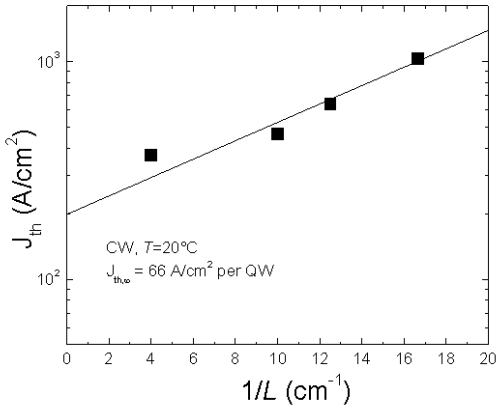

Figure 3 CW threshold current density as a function of inverse cavity length, at 20°C. No facet coating has been applied to this device.

For CW threshold characterization, devices were also episide-up mounted on copper heatsinks and facets were left uncoated. Threshold current as a function of inverse cavity length, under CW operation is plotted in Fig. 3. Very low threshold current densities of 66 A/cm^2 per QW have been extrapolated from the threshold current dependence on cavity length in Fig. 3. Since for previously published devices the data on threshold current at infinite length is not available, we have compared the values reported for certain resonator lengths, as can be seen in Table 1. One can see, that our value of 155 A/cm^2 per QW, for a 1 mm device with uncoated facets is better than the best reported value for episide-down mounted 2 mm device with HR/AC coatings up to now [12-13] and more than 3 times lower than values reported in [10] and [11].

In order to investigate the maximum operation temperature range under CW operation, we have applied a HR coating on one facet, resulting in a 95 % reflectivity and the other facet was left as cleaved. Episide-up mounted devices showed lasing up to a record-high heatsink temperature of 64 °C (see Fig. 4). This is by far the best reported value up to now. It is by 30 % better than the best value achieved for episide-down indium-soldered devices [12-13] and by a factor 2 better than the value reported in [10] and [11].

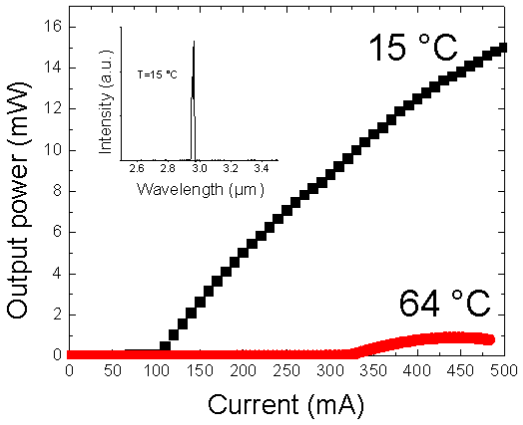

Figure 4 CW power-current characteristics of a 2 mm long device with a 7 μm wide mesa at 15 °C (black squares) and at 64 °C (red circles). The inset shows laser emission spectra at 15 °C.

We attribute such excellent device performance to a good epitaxial quality of the laser structures, indicated by a very low value of 3 cm^{-1} for intrinsic loss at 20 °C, and to the choice of well-barrier material combination, which enabled the achievement of high (71 meV) heavy-hole offsets, resulting in reduced hole leakage and improved temperature performance. Moreover, our quinternary barrier resulted in a lower conduction band offset (147 meV) than the one achieved with binary GaSb barriers (300 meV), what allowed a more homogeneous filling of the quantum wells and was reflected in very low threshold current densities.

ISBN 978-3-8007-3356-9

4 Conclussions

To summarize, we presented 3QW ridge waveguide lasers with record performance. The devices operate in CW mode up to record-high 64 °C and above 80°C in pulsed mode, with an emission wavelength in the range of 2.9 – 3.0 μm. They exhibit very low threshold current densities of 66 A/cm^2 and 56 A/cm^2 per QW for infinite length, at 20 °C in CW and pulsed operation, respectively. For this wavelength range, the presented devices have a very high characteristic temperature of 43 K. Such excellent performance is attributed to the fact that by using quinternary AlGaInAsSb barriers we were able to suppress hole leakage and increase the homogeneity of electron filling in the quantum wells by increasing heavy hole confinement to 71 meV and reducing the conduction band offsets to 147 meV.

5 Literature

[1] A. Vicet, D.A. Yarekha, A. Pérona, Y. Rouillard, S. Gaillard and A.N. Baranov, *Spectrochimica Acta Part A*, vol. 58, pp. 2405-2412, (2002).

[2] L. Rothman et al., 'The HITRAN 2004 molecular spectroscopic database', *J. Quant.Spectrosc. Radiat. Transf. ,* vol. 96, pp. 139 – 205, 2005.

[3] Y. Wang, H. S. Djie, B. S. Ooi, *J. Appl. Phys.*, vol. 98, 073508, (2005).

[4] Y. Wang, H. S. Djie, B. S. Ooi, P. Rotella, P. Dowd, V. Aimez, Y. Cao, Y. H. Zhang, *Thin Sol. Films*, vol. 515, pp. 4352-4355, (2007).

[5] O. Dier, S. Dachs, M. Grau, C. Lin, C. Lauer and M.-C. Amann, *Appl. Phys. Lett.*, vol. 86, No. 15, 151120, (2005).

[6] V. Sorokin, S. Sorokin, A. Semenov, B. Meltser and S. Ivanov, *J. Cryst. Growth*, vol. 216, pp. 97-103, (2000).

[7] I. Vurgaftman, J. R. Meyer and L. R. Ram-Mohan, *J. Appl. Phys.,* vol. 89, No. 11, pp. 5815 – 5875, (2001).

[8] G. P. Donatti, R. Kaspi and K. J. Malloy, *J. Appl. Phys.,* vol. 94, No. 9, pp. 5814 – 5819, (2003).

[9] M. Grau, C. Lin, O. Dier and M.-C. Amann, *Electron. Lett.*, vol. 39, No. 25, 20031216, (2003).

[10] S. Belahsene, L. Naehle, M. Fischer, J. Koeth, G. Bossier, P. Grech, G. Narcy, A. Vicet and Y. Rouillard, *IEEE Photon. Technol. Lett.,* vol. 22, No. 15, pp. 1084 – 1086, 2010.

[11] T. Lehnhardt, M. Hümmer, K. Rössner, M. Müller, S. Höftling, and A. Forchel, *Appl. Phys. Lett.,* vol. 92, pp. 183508, 2008.

[12] T. Hosoda, G. Kipshidze, L. Shterengas, S. Suchalkin and G. Belenky, *Appl. Phys. Lett.,* vol. 94, pp. 261104, 2009.

[13] T. Hosoda, G. Kipshidze, G. Tsvid, L. Shterengas, and G. Belenky, *IEEE Photon. Technol. Lett.,* vol. 22, No. 10, pp. 718 – 720, 2010.

ISBN 978-3-8007-3356-9